

Weakly Supervised Universal Fracture Detection in Pelvic X-rays

Yirui Wang¹, Le Lu¹, Chi-Tung Cheng², Dakai Jin¹, Adam P. Harrison¹,
Jing Xiao³, Chien-Hung Liao², Shun Miao¹

¹PAII Inc., Bethesda, MD, USA

²Chang Gung Memorial Hospital, Linkou, Taiwan, ROC

³Ping An Technology, Shenzhen, China

Abstract. Hip and pelvic fractures are serious injuries with life-threatening complications. However, diagnostic errors of fractures in pelvic X-rays (PXR) are very common, driving the demand for computer-aided diagnosis (CAD) solutions. A major challenge lies in the fact that fractures are localized patterns that require localized analyses. Unfortunately, the PXR residing in hospital picture archiving and communication system do not typically specify region of interests. In this paper, we propose a two-stage hip and pelvic fracture detection method that executes localized fracture classification using weakly supervised ROI mining. The first stage uses a large capacity fully-convolutional network, *i.e.*, deep with high levels of abstraction, in a multiple instance learning setting to automatically mine probable true positive and definite hard negative ROIs from the whole PXR in the training data. The second stage trains a smaller capacity model, *i.e.*, shallower and more generalizable, with the mined ROIs to perform localized analyses to classify fractures. During inference, our method detects hip and pelvic fractures in one pass by chaining the probability outputs of the two stages together. We evaluate our method on 4 410 PXR, reporting an area under the ROC curve value of 0.975, the highest among state-of-the-art fracture detection methods. Moreover, we show that our two-stage approach can perform comparably to human physicians (even outperforming emergency physicians and surgeons), in a preliminary reader study of 23 readers.

Keywords: Fracture classification and localization, Pelvic X-ray, Weakly supervised detection, Cascade two-stage training, Image level labels

1 Introduction

Hip and pelvic fractures belong to a frequent trauma injury category worldwide [8]. Frontal pelvic X-rays (PXR) are the standard imaging tool for diagnosing pelvic and hip fractures in the emergency room (ER). However, anatomical complexities and perspective projection distortions contribute to a high rate of diagnostic errors [2] that may delay treatment and increase patient care cost,

morbidity, and mortality [10]. As such, an effective PXR computer-aided diagnosis (CAD) approach for *both* pelvic and hip fractures is of high clinical interest, with the aim of reducing diagnostic errors and improving patient outcomes.

Image-level labels are the only supervisory signal typically available in picture archiving and communication system (PACS) data. Thus, a widely adopted formulation for X-ray abnormality detection is a single-stage global classifier [1, 3, 9, 11]. However, for PXRs this approach is challenged by the localized nature of fractures and the complexity of the surrounding anatomical regions. Moreover, such global classifiers can be prone to overfitting, as it is unlikely that a training dataset could capture the combinatorial complexity of configurations of fracture locations, orientations, and background contexts within the whole PXR—this complexity is analogous to similar challenges within computer vision [13]. Indeed, for *hip fractures alone*, Jiménez-Sánchez *et al.* show that using localized region of interests (ROIs) produces significantly better F1 scores over a global approach [7] and Gale *et al.* achieve impressive areas under the ROC curve (AUCROCs) of 0.994 by first automatically extracting ROIs centered on the femoral neck [4]. These recent results bolster the argument for concentrating on local fracture patterns.

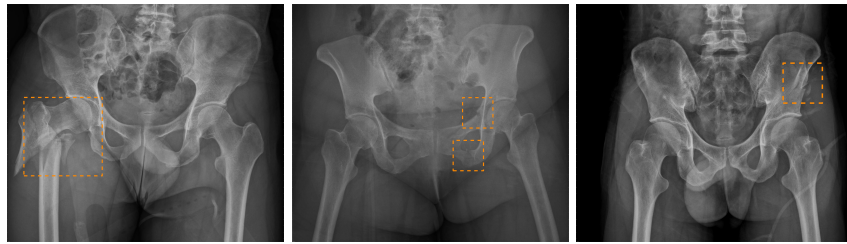


Fig. 1: Example PXR images of hip and pelvic fractures. **(Left)** Hip fracture. **(Middle)** Superior and inferior pubic ramus fracture. **(Right)** Iliac wing fracture.

Nonetheless, the above prior work all only focuses on diagnosing hip fractures and does not attempt to classify the more complex pelvic fractures (fractures in three pelvic bones: the ilium, ischium, and pubis). As Fig. 1 illustrates, the makeup of pelvis fractures is much more complex, as there are a large variety of possible types with very different visual patterns at various locations. In addition, pelvic bones overlap with the lower abdomen, further confounding image patterns. Finally, unlike hip fractures, which occur at the femoral neck/head, pelvic fractures can occur anywhere on the large pelvis, both increasing the aforementioned image pattern combinatorial complexity and precluding automatic ROI extraction based on anatomy alone, such as was done in prior work [4]. Thus, while using ROI-based classification is even more desirable for pelvic fractures, it is paradoxically more challenging to extract said ROIs.

To bridge this gap, we propose a two-stage weakly supervised ROI mining and subsequent classification method for PXR fracture classification. In the first

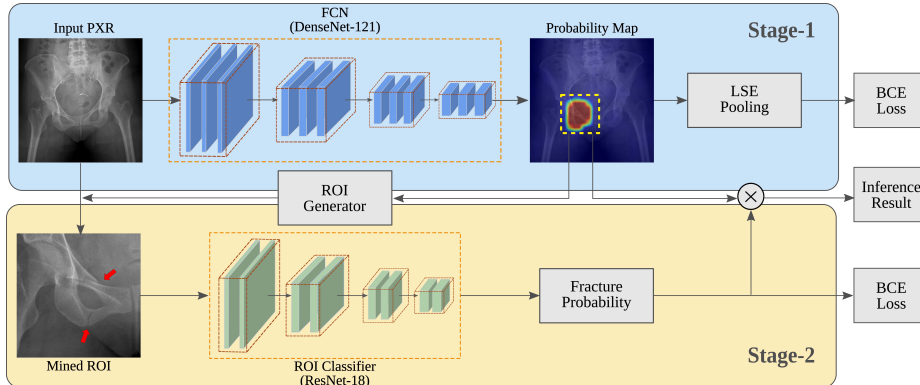


Fig. 2: The proposed two-stage fracture detection system. The first stage uses a large capacity MIL FCN model to perform fracture classification with weakly supervised ROI localization. The second stage uses a smaller capacity model trained with the mined ROIs to perform localized classification. During inference, the two stages are chained together, with the second model applied on the ROIs proposed by the first model, to produce the final estimation.

stage, we train a weakly-supervised, but high capacity, multiple instance learning (MIL) fully-convolutional network (FCN) to mine local probable positive and definite hard negative ROIs. In the second stage, we use the mined ROIs to train a lower capacity network in a fully-supervised setting. During inference, the two networks are chained together to provide a complete classification solution. Experiments use a dataset of 4 410 PXR, with only image-level labels, that we collected from the PACS of Chang Gung Memorial Hospital. We show that single-stage classifiers, whether low- or high-capacity, are unable to match our two-stage approach. Our chained two-stage method outperforms the best single-stage alternative, with a specificity at recall rate of 95% (S@R95) of 87.6% compared to 80.9%, and corresponding improvements in AUCROCs. Moreover, using an independent reader study of 150 patients, our system achieves an accuracy of 0.907, which is equivalent to 23 physicians. As such, we are the first to tackle automatic PXR pelvis fracture classification and also the first to demonstrate diagnostic performance equivalent to human physicians for *both* hip and pelvic fractures.

2 Method

Fig. 2 depicts the overall workflow of our chained two-stage pelvic and hip fracture detection method. We elaborate on the two stages below.

2.1 Weakly-Supervised ROI Mining

In the first stage, we train an FCN using a deep MIL formulation [12], employing the large-capacity DenseNet-121 [6] network as backbone. The DenseNet-121

features are then processed using a 1×1 convolutional layer and a sigmoid activation to produce a probability map. Owing to the localized properties of FCNs, each value of the probability map can be interpreted as the probability of fracture in the corresponding region in the input PXR. The maximum value would then represent the probability of fracture within the entire image. Instead, we use log of the sum of the exponentials (LSE) pooling, which is a differentiable approximation of max pooling, given by

$$LSE(S) = \frac{1}{r} \cdot \log \left[\frac{1}{|S|} \cdot \sum_{(i,j) \in S} \exp(r \cdot p_{ij}) \right], \quad (1)$$

where $\{p_{ij}\}$ is the probability map, and r is a hyper-parameter controlling the behavior of LSE between max pooling ($r \rightarrow \infty$) and average pooling ($r \rightarrow 0$). With the pooled global probability, binary cross entropy (BCE) loss is calculated against the image level label, and is used to train the network. While, this formulation has been applied directly for weakly supervised abnormality detection in chest X-rays (CXRs) [12], as we show in our results this approach’s performance is limited for hip and pelvic fracture detection. Therefore, we use the FCN as a proposal generator to mine ROIs from the training data.

To mine ROIs from the training data to train a localized classification model, we first create an image-level classifier using $p' = \max_{i,j \in S} p_{ij}$, and select a threshold \hat{p} corresponding to a high sensitivity on the training data (we use 99% in our experiments). We then extract up to $K = 5$ ROIs from each PXR in the training data in every training epoch of the second stage model. Specifically, for PXRs with positive ground-truth image-level labels, *i.e.*, with fracture(s), up to K locations are randomly selected from

$$S' = \{i, j | p_{ij} > \hat{p}\}. \quad (2)$$

These ROIs are labeled as probable fracture positive. For PXRs with negative ground-truth image-level labels, *i.e.*, no fractures, the same ROI extraction strategy selects up to K ROIs. These are considered as definite hard negatives. If there are less than K hard negatives extracted, additional negative ROIs are randomly extracted from the PXR to make up the total. The ROIs produced using the above strategy contains probable positives, hard negatives, and easy negatives. Although this approach adds a degree of label noise due to the probable positive ROI, as we outline in the following, this comes with the added benefits of using a subsequent localized and more generalizable ROI classifier.

2.2 Fracture ROI Classification

In the second stage, we use the ROIs mined from the first stage as training data for a fully supervised localized classification network. Since the positive samples are mostly ROIs around fractures with limited background context, the visual patterns of fractures become more dominant, simplifying the classification task. In addition, the distribution of mined ROIs are heavily weighted toward

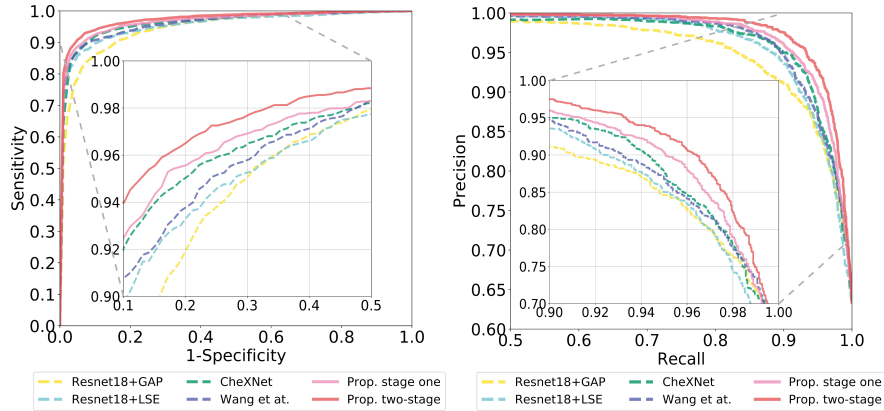


Fig. 3: Comparison of ROC (left) and Precision-Recall curve (right)

hard negatives, *i.e.*, false positive regions from the first stage. This concentrates the modeling power of the second-stage classifier on differentiating these difficult/confusing fracture-like patterns. As a result, we are able to train a smaller capacity network, *e.g.*, ResNet-18 [5], to reliably classify the ROIs, which is more generalizable and less prone to overfitting compared to a high-capacity network modeling the entire PXR.

During inference, the two stages are chained together to provide a complete solution. The first stage FCN acts as a proposal generator, and the highest value from the probability map $\{p_{i,j}\}$ is selected, denoted as p_{s1} , along with the corresponding ROI. The second stage classifier is then applied on the proposed ROI to produce a fracture probability score, denoted p_{s2} . The final image-level probability of fracture is computed by multiplying the two probability scores, $p_{s1} \cdot p_{s2}$. As such, we use the second stage classifier as a filter to reject false positives from the first stage.

Hip/pelvic fracture differentiation: Our two-stage method detects hip and pelvic fractures as one class, because the most important goal of PXR CAD is to detect fractures. Using one universal fracture class also helps to prevent the model from picking up co-occurrence relationships between hip/pelvic fractures that may be overly represented from the current training data [13]. In scenarios where hip and pelvic fractures do need to be differentiated, *e.g.*, automatic medical image reporting, an additional classification output node can be added to the second stage model. Similar to the hierarchical classification schemes [3], the new node is trained only on positive fracture ROIs mined in the first stage. Like fracture classification, during inference hip/pelvic fracture differentiation can be obtained in one feed-forward pass of the network.

Table 1: Five-fold cross validation of fracture classification on 4410 PXR.

Method	AUC	S@R95	R@S95	P@R95
ResNet18-GAP	0.946	0.706	0.786	0.846
ResNet18-LSE	0.956	0.723	0.859	0.851
CheXNet [9]	0.962	0.809	0.870	0.876
Wang <i>et al.</i> [11]	0.962	0.752	0.875	0.867
Prop. single-stage	0.968	0.825	0.888	0.903
Prop. two-stage	0.975	0.876	0.909	0.928

3 Experiments and Results

We evaluate our framework using PXR images collected from the PACS of Chang Gung Memorial Hospital, corresponding to patients in the trauma registry. We resized all images to 961×961 pixels. The final dataset consisted of 4410 images, including 2776 images with fractures (1975 and 801 hip and pelvic fractures, respectively). Besides this dataset, we also collected an independent PXR dataset, containing 150 cases (50 hip fractures, 50 pelvic fractures, and 50 no findings) for a reader study comparing our approach with that of 23 physicians.

We use ImageNet pre-trained weights to initialize the networks in both stages. The Adam optimizer was used to train both models for 100 epochs with a batch size of 8 and a starting learning rate of 10^{-5} reduced by a factor of 10 upon plateaus. In addition to AUCROC, we measure specificity at recall rate of 95% (S@R95), precision at recall rate of 95% (P@R95) and recall at specificity rate of 95% (R@S95), which help highlight differences in performance under demanding expectations for recall/sensitivity and specificity, respectively.

3.1 Comparison to Prior Work

We evaluate *general fracture* classification performance using five-fold cross-validation with a 70%/10%/20% training, validation, and testing split, respectively. We compare against the single-stage high-capacity approaches of CheXNet [9] and Wang *et al.* [11], both of which use DenseNet-121 as backbones and apply global average pooling (GAP) and LSE pooling, respectively. Note, that unlike our first stage of §2.1, the pooling is applied to the last feature map. We also compare against the single-stage lower-capacity model of ResNet-18, using both GAP and LSE pooling heads.

Fig. 3 and Tbl. 1 quantitatively summarizes these experiments. As can be seen, all lower-capacity models fare relatively poorly, demonstrating the need to use more descriptive models for global PXR interpretation. On the other hand, the first stage of our proposed method achieves an AUCROC of 0.968, compared to the 0.962 achieved by the state-of-the-art single-stage methods [9, 11], demonstrating that our single-stage approach using deep MIL can already outperform prior art. With the second stage, our method was able to further

Table 2: Algorithm and physician performances in a clinical study on 150 PXR.

	Accuracy	Hip Fracture		Pelvic Fracture	
		Sensitivity	Specificity	Sensitivity	Specificity
ER physician	0.881	0.983	0.937	0.813	0.955
Surgeon	0.855	0.931	0.928	0.829	0.932
Orthopedics specialist	0.932	1.000	0.953	0.905	0.990
Radiologist	0.930	0.990	0.965	0.870	0.995
Physician average	0.882	0.962	0.938	0.842	0.953
Our method	0.907	0.960	0.980	0.840	0.960

improve the AUCROC to 0.975, the highest among all evaluated methods. This corresponds to improvements of 12.4% (3.4%), 6.7% (3.9%), and 5.1% (2.1%) in S@R95 (R@S95) over Wang *et al.* [11], CheXNet [9], and our single-stage model respectively. These are highly impactful boosts in performance, demonstrating that under high demands of recall and specificity our chained approach can provide drastic improvements.

At our two-stage method achieves a P@R95 of 0.928, measuring 9.7%, 9.0%, 5.9% and 7.0% improvements over the two low-capacity baseline models, ResNet18-GAP and ResNet18-LSE, and two high-capacity baseline models CheXNet [9] and Wang *et al.* [11], respectively. Please note that the actual prevalence of fractures in clinical environments can be lower than our data, which will result in lower precisions for all methods. Nonetheless, the performance ranking would likely to remain, and the improvements of our method over the baselines are expected to be even more significant with a lower prevalence.

In addition, we evaluate the label accuracy of mined probable positive ROIs on 438 PXR with fracture location annotations, and report a high accuracy of 0.925, demonstrating the effectiveness of the proposed weakly-supervised ROI mining scheme. We also evaluate the hip/pelvic fracture classification performance, and report a high average accuracy of 0.980 over the five-fold cross validation.

3.2 Reader Study

We conduct reader study to compare performance on 150 PXR with 23 human physicians recruited from the surgical (11), orthopedics (4), ER (6) and radiology (2) departments. For every PXR, physicians were asked to choose from three options: hip fracture, pelvic fracture or no finding. To provide a fair comparison, we used the add-on fracture-type classification output node described in §2.2, which can differentiate between hip and pelvic fractures, matching the three-class classification performed by the readers.

Tbl. 2 quantitatively summarizes the reader study results. As shown in the results, our method performs comparably to the average physician performance on this dataset, reporting an accuracy of 0.907 compared to 0.882, with higher

levels of specificity. Examining the physician specialities in isolation, our method outperforms ER physicians and surgeons, while not performing as well as the orthopedic specialists and radiologists. Of note, is that when trauma patients are sent to the ER, it is common that only ER physicians or surgeons are available to make immediate diagnostic and treatment decisions. As such, the reader study suggests that our approach may be an effective aid for PXR fracture diagnosis in the high-stress ER environment.

4 Conclusion

We introduced a chained two-stage method for universal fracture detection in PXRs, consisting of a weakly supervised fracture ROI mining stage and a localized fracture ROI classification stage. Experiments show that our method can significantly outperform prior works via five-fold cross validation on 4410 PXRs. Moreover, a preliminary reader study on 150 PXRs involving 23 physicians suggests that our method can perform equivalently to human physicians. Thus, our approach represents an important step forward in automated pelvic and hip fracture diagnosis for ER environments.

References

1. Badgeley, M.A., Zech, J.R., Oakden-Rayner, L., et al.: Deep learning predicts hip fracture using confounding patient and healthcare variables. arXiv:1811.03695 (2018)
2. Chellam, W.: Missed subtle fractures on the trauma-meeting digital projector. *Injury* **47**(3), 674–676 (2016)
3. Chen, H., Miao, S., Xu, D., Hager, G.D., Harrison, A.P.: Deep hierarchical multi-label classification of chest x-ray images. *MIDL* (2019)
4. Gale, W., Oakden-Rayner, L., Carneiro, G., Bradley, A.P., Palmer, L.J.: Detecting hip fractures with radiologist-level performance using deep neural networks. arXiv:1711.06504 (2017)
5. He, K., Zhang, X., Ren, S., Sun, J.: Deep residual learning for image recognition. In: *Proceedings of the IEEE conference on computer vision and pattern recognition*. pp. 770–778 (2016)
6. Huang, G., Liu, Z., Van Der Maaten, L., Weinberger, K.Q.: Densely connected convolutional networks. In: *IEEE CVPR*. pp. 4700–4708 (2017)
7. Jiménez-Sánchez, A., Kazi, A., Albarqouni, S., Kirchhoff, S., Sträter, A., Biberthaler, P., Mateus, D., Navab, N.: Weakly-supervised localization and classification of proximal femur fractures. arXiv:1809.10692 (2018)
8. Johnell, O., Kanis, J.: An estimate of the worldwide prevalence, mortality and disability associated with hip fracture. *Osteoporosis International* **15**(11), 897–902 (2004)
9. Rajpurkar, P., Irvin, J., Zhu, K., Yang, B., Mehta, H., Duan, T., Ding, D., Bagul, A., Langlotz, C., Shpanskaya, K., et al.: Chexnet: Radiologist-level pneumonia detection on chest x-rays with deep learning. arXiv preprint arXiv:1711.05225 (2017)
10. Tarrant, S., Hardy, B., Byth, P., Brown, T., Attia, J., Balogh, Z.: Preventable mortality in geriatric hip fracture inpatients. *The bone & joint journal* **96**(9), 1178–1184 (2014)

11. Wang, X., Peng, Y., Lu, L., Lu, Z., Bagheri, M., Summers, R.M.: Chestx-ray8: Hospital-scale chest x-ray database and benchmarks on weakly-supervised classification and localization of common thorax diseases. In: IEEE CVPR (2017)
12. Yao, L., Prosky, J., Poblenz, E., Covington, B., Lyman, K.: Weakly supervised medical diagnosis and localization from multiple resolutions. arXiv preprint arXiv:1803.07703 (2018)
13. Yuille, A.L., Liu, C.: Deep nets: What have they ever done for vision? CoRR **abs/1805.04025** (2018)